Expressing remorin in animal cells forms filamentous structure unraveling the mechanism of plasmodesmata biogenesis

Authors: Zhuang Wei[1‡], Shu-Tang Tan[2‡], Tao Liu[1, 3‡] Yuan Wu[1, 3], Ji-Gang Lei[1, 3], Hong-Wei Xue[2, 4*†], Kan Liao[1*†]

Affiliations:

[1]Key Laboratory of Systems Biology, CAS Center for Excellence in Molecular Cell Science, Shanghai Institute of Biochemistry and Cell Biology, Chinese Academy of Sciences, Shanghai 200031, China

[2]National Key Laboratory of Plant Molecular Genetics, CAS Center for Excellence in Molecular Plant Sciences, Shanghai Institute of Plant Physiology and Ecology, Chinese Academy of Sciences, 200032 Shanghai, China

[3]University of Chinese Academy of Sciences

[4]School of Agriculture and Biology, Shanghai Jiao Tong University, 200240 Shanghai, China

*Correspondence should be addressed to K.L. (kliao@sibs.ac.cn) and X.H. (hwxue@sibs.ac.cn)

‡W.Z., T.S. and L.T. contributed equally to this work.

†L.K. and X.H. contributed equally to this work.

Running title: Remorin and plasmodesmata biogenesis

Key words: plasmodesmata; biogenesis; Remorin; vesicle; migrasome

Summary

Plants plasmodesmata (PD) are important structures for plant. The biogenesis of PD is an important and poorly understood process. Remorin is a highly conserved PD protein, but its contribution to the formation of PD is difficult to study because of the redundancy of remorin in plants and the importance of PD for plant cell survival. We found expression of remorin in animal cells mimics a functional PD-like structure by deforming the membranes into filamentous vesicles. After systematic verification and comparison studies, we found remorin converts the animal cell membrane into remorin filaments (RFs). Interestingly, these PD-like remorin filaments are similar to the migrasome, a kind of material transfer structure on the surface of animal cells, from multiple aspects. Our studies not only reveal the mechanism of PD biogenesis, but also explain the fundamental links of intercellular transport systems between plants and mammals. In addition, the unique character and effect of remorin indicate the potential biomedical applications.

Introduction

The PD system is generally considered to be an essential difference between animal and plant cells (Maule, 2008). However, the molecular basis underlying the PD biogenesis remains unclear. Migrasome is a strip-like cell structure that is produced during cell migration and functions as a substance transporter(Ma et al., 2015). Interestingly, various clues suggest that PD and migrasome are very similar, because they are all vesicle structures on cell surface, all composed of lipid microdomains, and are all closely related to the interaction of the cytoskeleton and cell membrane(Marín and Ott, 2012, Bariola et al., 2004, Ma et al., 2015). Based on the similarities between PD and migrasome, we speculate that a distinct protein Remorin, a plant-specific protein located at the PD (Kronberg et al., 2007) that marks the lipid microdomain or nanodomain (Jarsch and Ott, 2011, Marín and Ott, 2012, Raffaele et al., 2009, Perraki et al., 2014, Gui et al., 2014), is responsible for transforming membrane into migrasome-like. Studying this can not only explain the biogenesis of PD of plant, but also can explain why animal cells lack PD at the molecular level.

Here, we investigated heterologously expressed remorin in mammalian cells leads to the formation of plant PD-like structure (Remorin filaments RFs). Our study indicates that a single protein, remorin, is sufficient to constitute a PD-like structure in two eukaryotic cells and reveals the evolutionary difference in intercellular communication between animals and plants.

Results

Deficiency of remorin leads to PD abnormality in *Arabidopsis*

In *Arabidopsis*, the remorin family has 16 isoforms, of which remorin1.2 (REM1.2, AT3G61260) and remorin1.3 (REM1.3, AT2G45820) show high similarities and were reported to be localized at the PD (Raffaele et al., 2009). To confirm the role of remorin in PD formation and function, we obtained T-DNA insertional mutants, *rem1.3* from the *Arabidopsis* Biological Resource Centre (ABRC) and *rem1.2* via Cas9-mediated mutagenesis (Fig 1A). The rosette size of the double knock-out mutant (*DKO*, *rem1.3 rem1.2*) is smaller than that of the wild-type (WT), with tiny leaves (Fig 1C, S1 A-C), indicating that REM1.2 and REM1.3 are essential for plant growth. Thus, it is hypothesized that loss of function of REM1.2 and REM1.3 might affect the physiological function of PD. PD play an important role in transporting different molecules, including carbohydrates in plant cells (Brunkard et al., 2015, Burch-Smith and Zambryski, 2012). Consistently, a starch unloading experiment is a classical and persuasive method for systematically detecting the ability of *Arabidopsis* to transport sugars via PD (Lee et al., 2011). The results showed that there was almost no detectable accumulation of starch in the leaves of the WT, whereas 51% of the leaves of the *DKO* had a significantly positive starch accumulation (Fig. 1D).

To confirm the function of REM1.2 and REM1.3 in PD, we tested PD permeability with a fluorescent dye, FDA (fluorescein diacetate) (Gui et al., 2015, Gui et al., 2014). FDA was pre-infiltrated into plants and then bleached by a strong laser. Finally, the recovery rate of the FDA fluorescence was measured. As shown in Fig. 1E, *Arabidopsis* WT plants recovered more rapidly than the *DKO* plants (WT, 70%; *DKO*, 30% at 290 s). This demonstrates that FDA diffusion is more difficult in the *DKO* plants, confirming the crucial role of REM1.2 and REM1.3 in the physiological function of the PD.

Further detailed analysis with TEM (transmission electron microscopy) indicated that the number of PD was significantly decreased in the mutants (Fig 1F; WT, 5.4; *rem1.3-1*, 4.0; *rem1.2-1*, 2.1; *DKO*, 1.8). However, several dark osmiophilic globules (~ 50 nm in size) were observed in the *rem1.3* and *rem1.2* cells, with a greater number in the *DKO* cells (Fig 1F), which is probably due to PD dysfunction (Sehnke et al., 2001, Kawasaki et al., 1999). Thus, REM1.2 and REM1.3 are crucial in PD biogenesis and thus in plant growth.

Heterologous expression of remorin enables mammalian cells to exchange

macromolecules

To dispel the concern that remorin expression in animal cells is incorrect, we analyzed the basic biochemical properties of remorin in animal cells. Remorin was previously reported to localize at certain lipid microdomains (Jarsch and Ott, 2011, Marin et al., 2012, Raffaele et al., 2009, Perraki et al., 2014, Gui et al., 2014). In parallel with the previous results, remorin isoforms (REM1.2, REM1.4 and REM1.1) can be expressed in mammalian cells and is associated with the lipid microdomains through sucrose-density gradient centrifugation (Fig S2A). Remorin is also reported to be post-translationally modified by palmitoylation (Konrad et al., 2014). We employed an acyl-biotin exchange assay to detect the palmitoylation of REM1.3. The results showed that wild-type REM1.3 expressed in mammalian cells can be palmitoylated (Fig S2B). These results showed that heterologously expressed REM1.3 in mammalian cells presents the same subcellular localization and biochemical modification as in plant cells.

The function of PD in plants is to communicate through biomolecules between cells (Brunkard et al., 2015, Burch-Smith and Zambryski, 2012). To investigate whether remorin is a determinant of PD formation, we used a Cre-LoxP system to test whether heterologous expression of remorin in animal cells can result in communication/transport of material between cells to mimic the PD function. A set of highly sensitive detection systems was designed (Fig 2A). Analysis by fluorescence microscopy and flow cytometry showed that donor cells expressing remorin and an ER-localized Cre recombinase enabled the receptor cells to exhibit GFP fluorescence, while non-ER-localized Cre recombinase or a lack of remorin expression in the donor cells exhibited no detectable signal (Fig 2B and C). This result confirms that remorin expression in the donor cells can transmit Cre recombinase to the receptor cell.

To verify the molecular basis for remorin connecting animal cells, we observed the localization of eGFP-tagged REM1.3 in cells by confocal microscopy. As shown in Fig 2D and E, eGFP-REM1.3 distributed at some filamentous structures (termed remorin filaments, RFs) across the cell. Interestingly, both ends of the RFs were swelling, with positive staining of the endoplasmic reticulum marker protein calnexin (Lynes et al., 2013). This is especially common when the cell density is low. A schematic diagram of RFs across two cells (Fig 2D) is a typical structural feature for plant PD, and this type of RF structure is possibly similar to the structure of plant PD.

To observe and confirm that remorin connects two cells more directly, we infected primary myocardial cells using the eGFP-REM1.3 adenovirus. As shown in Fig 2F, the number of eGFP-REM1.3 filamentous structures linked to cardiomyocytes (connectors) was greater than that for the control (empty vector) cells. Because primary myocardial cells have a rhythmic impulse, it is possible to demonstrate that two cells or cell populations are connected if they have consistent rhythms. Simultaneous video analysis illustrated that two linked cells or cell populations share a synchronous beat rhythm (Fig 2G), confirming that ions pass through the two groups of cardiomyocytes through the RFs.

Identification of RFs in mammalian cells

To characterize the similarity between RFs and the plant PD and to explore their biogenesis, we performed a series of microscopic observations and biochemical experiments. As shown in Fig 3 and Table S1, RFs have a diameter of approximately 100-150 nm, one-tenth to half of a cell length, and are usually branched. Co-stained with different markers, RFs stained positive for phalloidin (actin filaments, AFs) and negative for α-tubulin (microtubule, MT, markers), vimentin (intermediate filament) and Fascin (filopodial markers), suggesting that RFs are AF-based (Fig 3 A-G and S3 A-E) (Svitkina et al., 2003). Cells treated with cytochalasin B (CBB), an AF-depolymerizing reagent, exhibited collapsed RFs (Fig 3B), confirming the physical interaction of actin and remorin, similar to plant PD (Brunkard et al., 2015, Burch-Smith and Zambryski, 2012).

The structure of PD was uncovered by cryo-electron microscopy (Burch-Smith and Zambryski, 2012). An AF spiral twining an ER tube and an electron dense spiral helix surrounding the AFs were observed. Using structured-illumination microscopy (SIM), a super-resolution microscopy, we evaluated the detailed structure of RFs. Refined images (Fig 3C) indicate that the two eGFP-remorin parallel spiral helices twin AFs with an external diameter of 103.34±5.95 nm and a pitch of 140.11±27.21 nm, which is further confirmed by quantification analysis (Table S1). We also used another super-resolution microscopy with a different principle from SIM, stochastic optical reconstruction microscopy (STORM). Both N-Storm (Fig 3D and S4) and C-Storm (Fig 3E) images show that RFs are spiral helices, coincident with the SIM result. These results provide further evidence confirming that RFs are indeed PD-like structures.

Moreover, a comprehensive transmission electron microscopy (TEM), which allows us to combine fluorescence imaging and TEM in the same sample by using a fluorescein and nano-gold particle double-labeled secondary antibody, clearly demonstrated that the fluorescence signal of RFs was observed as gold-particle-positive helical structures on TEM (Fig 3F). This further confirmed the spiral structure of RFs determined by super-resolution microscopy.

Functional characterization of the different remorin domains in mammalian cells

To study the biogenesis process of RFs, we investigated how the primary structure of REM1.3 contributes to RF formation in mammalian cells. Various truncated REM1.3s are expressed (Fig 4A and S5), and RF formation and lipid microdomain localization are observed to indicate the domain contribution. The function of each domain is summarized in Table S2.

Lack of the N-terminus of REM1.3 (CT) does not obviously affect the distribution pattern of remorin (Fig 4B and S6). When we truncated most of the N-terminus containing the coiled-coil domain (T) or truncated only four amino acids in the C-terminus (1-186), the distribution pattern of REM1.3 significantly changed into a disperse eGFP signal. Lipid microdomain localizations of these two truncated versions were also destroyed (Fig 4D and S7), indicating that the coiled-coil domain and the four amino acids in the C-terminus are essential for the formation of RFs. Consistently, a CC domain deletion mutation (ΔCC) could not form RFs (Fig 4A-C).

To study the contribution of the TLD domain (aa 150-186), we linked the four amino acids of the C-terminus directly to the N-terminus with the coiled-coil domain (NCP). This truncation showed a disperse distribution but did not affect the protein lipid microdomain localization. Further deletion of the N-terminal amino acids 1-76 (CP) showed a lipid microdomain distribution but, surprisingly, a small uniform punctate distribution in cells. Phalloidin staining demonstrated that those special structures are adjacent to, but not overlapping with, the F-actin dots (Fig 4B). These results suggest that the TLD domain contributes to the formation of the long RF helix and retains the ability to associate with actin oligomers as an initiative structure of RFs. The results also indicate that the N-terminus of REM1.3 is an inhibitory domain for RF formation.

To confirm that remorin indeed interacts with lipid microdomains like the animal vesicle system migrasome, we evaluated the expression of remorin by immunofluorescent staining of two major lipid microdomain proteins, caveolin-1 and cavin-1. The results showed that a large number of remorin signals co-localized with caveolin-1 and cavin-1; however, some of these signals did not form filamentous tips, suggesting that remorin and lipid microdomains are closely related (Fig 4E).

To further study the molecular mechanism of remorin binding to lipid microdomains and their contributions to the formation of RFs, we mutated cysteine 187 or 189 to alanine (Ala, A) or aspartic acid (Asp, D) separately or together. The distribution of REM1.3 changed to inclusion bodies in the cytoplasm (Fig S6), and the proteins disappeared from the lipid microdomains (Fig S7). This corresponded to the results from the palmitoylation study in Fig S2B. We also linked the four amino acids CGCF of the C-terminus of REM1.3 (aa 187-190) directly into the tail of eGFP; ~30% eGFP proteins were partially associated with the lipid microdomains (Fig S7) but showed a dispersed localization (Fig S6), which suggests that those four amino acids are sufficient to lead the protein onto the lipid microdomains.

The above results show the coiled-coil domains, TCHP-like domains and C-terminal palmitoylation of remorin are crucial for RF biogenesis. Thus, we hypothesize that remorin deforms the membrane raft into a filament-like structure. To directly observe the process, a video series was obtained using a video microscope. The results clearly indicated that the RFs budded out the vesicles, appearing to elongate (Fig 4F and G).

To further confirm that the knowledge obtained from animal cells can be validated in plants, we transformed different truncated versions of *REM1.3* driven by a CaMV35S promoter into WT *Arabidopsis*. The results showed that the full-length (FL) protein and the C-terminus (CT) localized at the plasma membrane (PM) without any nuclear signals (Fig S8). In contrast, truncation of the TLD domain (CP) showed a nuclear signals(Fig S8). Distribution in guard cells is a clearer indicator (Fig S8). These results are identical to those observed from animal cells.

Discussion

Remorin initiates and elongates plasmodesmata

Previous studies showed that remorin is involved in the physiological function of PD, but its mechanism is unclear, and the molecular machinery underlying PD biogenesis is largely unknown (Bariola et al., 2004, Gui et al., 2014, Konrad et al., 2014, Raffaele et al., 2007, Raffaele et al., 2009). Using a genetic approach, we demonstrated that remorin affected the connectivity of the PD. This confirms that Remorin is related to PD. However, it is still very difficult to study the molecular mechanism of Remorin in PD biogenesis from plants. Therefore, a brand new perspective was proposed, which is mammalian cells can be a fine model to investigate PD biogenesis and its related proteins. The logic is based on following reasons: Firstly, mammalian cells are well studied higher eukaryotic cells, which possess conserved cytoskeleton and membrane system parallel with plants. Secondly, mammalian cells are absent of cell walls, which ensures that we can easily observe and analyze the change of cytoskeleton and cell membrane interactions using leading-edge microscopy or other methods. Finally, mammalian cells are lack of PD and its related proteins, which provides low background to analyze the change.

To verify that the heterologously expressed remorin in animal cells could still maintain its known bioactivity, we first confirmed the lipid microdomain localization and palmitoylation of remorin. These characteristics are highly similar to those of remorin in plant cells (Gui et al., 2014, Konrad et al., 2014, Marin et al., 2012, Raffaele et al., 2009) and allow us to study remorin in animal cells.

By expressing remorin, we reconstitute functional PD-like structures. An ER-distributed protein is indeed transferred from donor cell to acceptor cell in the presence of remorin, which is very similar to the classic function of PD (Burch-Smith and Zambryski, 2012). This suggests that a single remorin protein is essential for the initiation and maintenance of the core PD structure. Furthermore, we identified the filamentous structure between two animal cells formed by remorin, i.e., a quadruple actin-remorin helix (=double actin helices × double remorin helices) skeleton for RFs (Fig 5A). Remorin filaments (RFs) are not any of the previously reported filamentous cell surface structures, such as cilia, flagella or intermediate filament (Konno et al., 2015). Although the filamentous structure formed by remorin consists of AFs, it is different from filopodia and tunneling-nanotubes (Svitkina et al., 2003). RFs do not have filopodia or tunneling-nanotube marker proteins (Rustom et al., 2004, Vignjevic et al., 2006, Svitkina et al., 2003). Moreover, RFs are swollen at both ends, which is different from the classic structure of tunneling-nanotubes, but it is very similar to the structure of a plasmodesma (Rustom et al., 2004).

More intrinsic mechanism research supports Remorin initiation and extension PD. The lack of coiled-coil domain, mutation of the cysteine at the C-terminal anchor and deletion of the TCHP-like domain (TLD) affect RF biogenesis. Removing the N-terminal domain from the TCHP-like-domain-lacking REM1.3 can still form the initiatory structure of RFs next to F-actin but results in RFs extending to a lesser degree. This can infer coiled-coil domains interact with F-actin and form an RF organization center near the cell membrane, which is responsible for RF initiation (Fig 5B). They The docking data based on Remorins predicted structure and the F-actin crystal structure (http://hexserver.loria.fr/) also support the above notion (Ghoorah et al., 2013). So TCHP-like domain is likely to be responsible for the extension of RF. During RF extension, lipid microdomains prolong spirally following remorin and the F-actin helix.

The similar results obtained from both plant and mammalian cells are mutually supportive; the conclusions drawn from the animal cells also gave predictable results for plant cells. Thus, it is speculated that plant PD have the same initial biogenesis process. The important functions of remorin during the biogenesis of PD include linking the cytoskeleton to the cell membrane and stretching it into a filamentous form.

We conclude that remorin filaments can be studied in animal cells as PD and state that remorin is a key evolutionary factor that is the major difference between the cellular transport systems of animals and plants.

Plant plasmodesmata and animal migrasome

Migrasome is a newly discovered long filamentous cell structure(Ma et al., 2015, Wu et al., 2017, Chen et al., 2018). It is related to the cell movement and plays a role in intercellular communication in animal cells. Migrasome has a filamentous structure with spherical protrusions on the filaments, and our RFs also have this feature, such as Fig 2D and E. Migrasome has been shown to be encapsulated into cytoplasmic components and released outside the cell, and we have observed this phenomenon in RFs, such as Fig 2E, which encapsulates intracellular substances such as DNA and endoplasmic reticulum. At the same time, the biochemical properties of RFs are similar to migrasome, which are rich in Actin and are lipid microdomains(Ma et al., 2015, Wu et al., 2017). Because the important concomitant ingrigrins of migrasome is also an important component of lipid microdomain(Babel et al., 2017). In summary, we believe that RFs have a very high similarity to migrasome. Therefore, it can be considered that migrasome on animal cells is an analog of PD on plants, the enlargement on migrasomes can be understood as a series of plant cells in series, and the pattern diagram is shown in Fig 5C. Although animal cells do not have cell walls and cannot be given a rigid adhesion platform that is as stable as plant PD, the migrasome is adhered to the bottom of the Petri-dish and the bottom of the Petri-dish can be considered a flat cell wall. The formation of Migrasome has been shown to be associated with extracellular matrices (ECM) and adhesion factors(Wu et al., 2017). In the future, using three-dimensional culture channels to simulate plant cell wall, it is possible to simulate PD that are more similar to plant cells on animal cells.

Potential biomedical application of remorin

Because remorin has the ability to form a physical connection between animal cells, we can envision using it for the delivery of large proteins or other molecules that are not readily transported by conventional methods into recipient cells. As a potent protein that affects cell-cytoskeletal interactions, exogenous expression of remorin may serve as a regulatory tool to explore the unobservable behavior of animal cells. For example, we observe a strong inhibition of zebrafish zygote cleavage upon heterologous expression of remorin protein via yolk injection (Fig S9), which suggests that remorin can be developed as a cell cleavage inhibitor with its actin modulation function for biomedical use.

References

BABEL, L., KRUSE, L., BUMP, S., LANGHANS, M. & MECKEL, T. 2017. Lipid-rafts remain stable even after ionizing radiation induced disintegration of beta1 integrin containing focal adhesions. *BMC Res Notes,* 10**,** 697.

BARIOLA, P., RETELSKA, D., STASIAK, A., KAMMERER, R., FLEMING, A., HIJRI, M., FRANK, S. & FARMER, E. 2004. Remorins form a novel family of coiled coil-forming oligomeric and filamentous proteins associated with apical, vascular and embryonic tissues in plants. *Plant molecular biology,* 55**,** 579-594.

BRUNKARD, J. O., RUNKEL, A. M. & ZAMBRYSKI, P. C. 2015. The cytosol must flow: intercellular transport through plasmodesmata. *Current opinion in cell biology,* 35**,** 13-20.

BURCH-SMITH, T. M. & ZAMBRYSKI, P. C. 2012. Plasmodesmata paradigm shift: regulation from without versus within. *Annual review of plant biology,* 63**,** 239-260.

CHEN, Y., LI, Y., MA, L. & YU, L. 2018. Detection of Migrasomes. *Methods Mol Biol,* 1749**,** 43-49.

GHOORAH, A. W., DEVIGNES, M.-D., SMAIL-TABBONE, M. & RITCHIE, D. W. 2013. Protein docking using case-based reasoning. *Proteins-Structure Function and Bioinformatics,* 81**,** 2150-2158.

GUI, J., LIU, C., SHEN, J. & LI, L. 2014. Grain setting defect1, encoding a remorin protein, affects the grain setting in rice through regulating plasmodesmatal conductance. *Plant physiology,* 166**,** 1463-1478.

GUI, J., ZHENG, S., SHEN, J. & LI, L. 2015. Grain setting defect1 (GSD1) function in rice depends on S-acylation and interacts with actin 1 (OsACT1) at its C-terminal. *Frontiers in plant science,* 6**,** 804.

JARSCH, I. K. & OTT, T. 2011. Perspectives on remorin proteins, membrane rafts, and their role during plant–microbe interactions. *Molecular plant-microbe interactions,* 24**,** 7-12.

KAWASAKI, M., MATSUDA, T. & NITTA, Y. 1999. Electron Microscopy of Plastid-Amyloplast System Involved in Starch Synthesis and Accumulation in Potato Tuber: Sloanum tuberosum L. *Japanese Journal of Crop Science,* 68**,** 266-274.

KONNO, A., SHIBA, K., CAI, C. & INABA, K. 2015. Branchial Cilia and Sperm Flagella Recruit Distinct Axonemal Components. *Plos One,* 10.

KONRAD, S. S., POPP, C., STRATIL, T. F., JARSCH, I. K., THALLMAIR, V., FOLGMANN, J., MAR N, M. & OTT, T. 2014. S ‐ acylation anchors remorin proteins to the plasma membrane but does not primarily determine their localization in membrane microdomains. *New Phytologist,* 203**,** 758-769.

KRONBERG, K., VOGEL, F., RUTTEN, T., HAJIREZAEI, M.-R., SONNEWALD, U. & HOFIUS, D. 2007. The silver lining of a viral agent: increasing seed yield and harvest index in Arabidopsis by ectopic expression of the potato leaf roll virus movement protein. *Plant physiology,* 145**,** 905-918.

LEE, J.-Y., WANG, X., CUI, W., SAGER, R., MODLA, S., CZYMMEK, K., ZYBALIOV, B., VAN WIJK, K., ZHANG, C. & LU, H. 2011. A plasmodesmata-localized protein mediates crosstalk between cell-to-cell communication and innate immunity in Arabidopsis. *The Plant Cell,* 23**,** 3353-3373.

LYNES, E. M., RATURI, A., SHENKMAN, M., SANDOVAL, C. O., YAP, M. C., WU, J., JANOWICZ, A., MYHILL, N., BENSON, M. D., CAMPBELL, R. E., BERTHIAUME, L. G., LEDERKREMER, G. Z. & SIMMEN, T. 2013. Palmitoylation is the switch that assigns calnexin to quality control or ER Ca2+ signaling. *Journal of Cell Science,* 126**,** 3893-3903.

MA, L., LI, Y., PENG, J., WU, D., ZHAO, X., CUI, Y., CHEN, L., YAN, X., DU, Y. & YU, L. 2015. Discovery of the migrasome, an organelle mediating release of cytoplasmic contents during cell migration. *Cell Res,* 25**,** 24-38.

MAR N, M. & OTT, T. 2012. Phosphorylation of intrinsically disordered regions in remorin proteins. *Frontiers in* *plant science,* 3**,** 86.

MARIN, M., THALLMAIR, V. & OTT, T. 2012. The Intrinsically Disordered N-terminal Region of AtREM1.3 Remorin Protein Mediates Protein-Protein Interactions. *Journal of Biological Chemistry,* 287.

MAULE, A. J. 2008. Plasmodesmata: structure, function and biogenesis. *Current Opinion in Plant Biology,* 11**,** 680-686.

PERRAKI, A., BINAGHI, M., MECCHIA, M. A., GRONNIER, J., GERMAN-RETANA, S., MONGRAND, S., BAYER, E., ZELADA, A. M. & GERMAIN, V. 2014. StRemorin1. 3 hampers Potato virus X TGBp1 ability to increase plasmodesmata permeability, but does not interfere with its silencing suppressor activity. *FEBS letters,* 588**,** 1699-1705.

RAFFAELE, S., BAYER, E., LAFARGE, D., CLUZET, S., RETANA, S. G., BOUBEKEUR, T., LEBORGNE-CASTEL, N., CARDE, J.-P., LHERMINIER, J. & NOIROT, E. 2009. Remorin, a solanaceae protein resident in membrane rafts and plasmodesmata, impairs potato virus X movement. *The Plant Cell,* 21**,** 1541-1555.

RAFFAELE, S., MONGRAND, S., GAMAS, P., NIEBEL, A. & OTT, T. 2007. Genome-wide annotation of remorins, a plant-specific protein family: evolutionary and functional perspectives. *Plant physiology,* 145**,** 593-600.

RUSTOM, A., SAFFRICH, R., MARKOVIC, I., WALTHER, P. & GERDES, H. H. 2004. Nanotubular highways for intercellular organelle transport. *Science,* 303**,** 1007-1010.

SEHNKE, P. C., CHUNG, H.-J., WU, K. & FERL, R. J. 2001. Regulation of starch accumulation by granule-associated plant 14-3-3 proteins. *Proceedings of the National Academy of Sciences,* 98**,** 765-770.

SVITKINA, T. M., BULANOVA, E. A., CHAGA, O. Y., VIGNJEVIC, D. M., KOJIMA, S.-I., VASILIEV, J. M. & BORISY, G. G. 2003. Mechanism of filopodia initiation by reorganization of a dendritic network. *J Cell Biol,* 160**,** 409-421.

VIGNJEVIC, D., KOJIMA, S.-I., ARATYN, Y., DANCIU, O., SVITKINA, T. & BORISY, G. G. 2006. Role of fascin in filopodial protrusion. *J Cell Biol,* 174**,** 863-875.

WU, D., XU, Y., DING, T., ZU, Y., YANG, C. & YU, L. 2017. Pairing of integrins with ECM proteins determines migrasome formation. *Cell Res,* 27**,** 1397-1400.

Acknowledgements:

This work was supported by National Natural Science Foundation of China [NSFC 31701165, 31370818, 31721001]; Ten-Thousand Talent Program.

Author contributions:

Z. W., S. T. proposed the initial idea of exogenous Remorin in animal cells. Z. W., S. T., K. L and H. X. designed the experiments. Z. W., S. T. and T. L. performed most of the experiments and data analysis. Z. W., S. T., K. L and H. X. wrote the manuscript. Z. W., T. L. carried out substances transport experiment in animal cells.

Figure Legends

Fig 1. Deficiency of remorin leads to PD abnormality in *Arabidopsis*.

A. A schematic diagram of the structures of *REM1.2* and *REM1.3* and the related mutants *rem1.3* and *rem1.2.*

B. Western blotting indicates knock-out of REM1.2 and REM1.3 in *rem1.2*, *rem1.3*, and *rem1.2 rem1.3* mutants using α-REM1.3 / 1.2 antibody, controlled by Coomassie blue staining.

C. The rosette size of *rem1.3. rem1.2* double mutant was smaller than that of WT. Thirty-day-old plants are shown. *rem1.3, rem1.2* and *DKO* (double knock-out).

D. Deficiency of remorin impairs starch transport in *Arabidopsis*. After 45 days of growth of wild-type WT, *rem1.3, rem1.2* and *DKO*, the plants were kept in the dark for 18 h. The leaves were fixed in ethanol and subjected to Loguls iodine staining . The blue-black portion indicates starch accumulation. The images on the right show the leaves without starch accumulation (WT) and starch accumulation (*DKO*) as standards. The bar chart shows the statistical result of starch accumulation (%). Four leaves were randomly selected from one plant, and the study was repeated on 15 plants per line.

E. Dye diffusion experiment for WT and *DKO*, 7-day-old plants were stained with 1 mM FDA solution for 2 minutes. Roots were used for a FRAP experiment under a laser confocal microscope. Heat map shows the fluorescence degree of recovery.

F. Remorin-knockout plants show a decrease of PD and an increase of osmiophilic particles. TEM images of remorin-KO plants. Upper panels are low-magnification images of WT, *rem1.3, rem1.2* and *DKO*; bottom panels are high-magnification images. Green and orange pseudo colors indicate the PD and osmiophilic particles. The bar chart presents the statistical result of the TEM images (PDs and Dots Numbers ± SD). Green and orange bars indicate the number of PD and deep dyeing globules in every two cells, respectively.

Fig 2. Exogenously expressed remorin enables animal cell-cell material transport.

A-C. Co-expression of remorin and endoplasmic-reticulum-located CRE recombinase (ERs-Cre) in donor cells, expression of “lmlg” (LoxP-mCherry-multiple stop codons-LoxP) elements in acceptor cells. The lmlg element is an expression box consisting of LoxP, mCherry, multiple stop codon sites, LoxP and GFP proteins in series. In the absence of Cre recombinase, only mCherry was expressed (red); in the presence of Cre recombinase, the mCherry and multi-stop codon sites in the middle of LoxP were excised, leading to expression of the GFP protein (green). The Cre recombinase was transfected into donor cells. If the proteins between the donor and recipient cells could communicate with/transport to each other, the lmlg element is cleaved by CRE, mCherry (mCr) and multiple stop codons are excised, and GFP begins to express, receptor cells with green fluorescence were expected to be visualized. After transfection for 48 hours, 1:1 mixed cells are cultured for 48 hours before observation by microscope (green: GFP; red: mCherry; blue: DNA: Bar = 100 μm), double-positive cell statistics conducted by flow cytometry with a bar chart [% Numbers of GFP positive / (GFP positive + mCherry positive) cells ± SD].

D. PD-like structure formed in animal cells transfected with eGFP-REM1.3 and stained for ER with calnexin antibody (red: Calnexin; green: REM1.3; blue: DNA; bar = 10 μm). The right portion shows PD-like structure pattern on animal cells (red: endoplasmic reticulum; green: cell body; blue: cell nucleus).

E. PD-like structure transports DNA from cell. Animal cells transfected with eGFP-REM1.3 (green: REM1.3; red: phalloidin stained F-Actin; pink: Calnexin; blue: DNA stained by diaminophenindole, DAPI; bar = 10 μm)

F. Mouse cardiac myocytes infected with eGFP-REM1.3 or eGFP control vector adenovirus (green: REM1.3 or eGFP-control; gray: bright field; bar = 200 μm).

G. Cell populations or cells that are connected together shown with a bar chart (Numbers of connectors per field ± SD). The pulsatile displacement of both cell clusters (red: A; blue: B) was recorded on the red and blue lines on Image Pro Plus software, respectively.

Fig 3. Remorin forms PD-like RFs in mammalian cells.

A. HEK293 cells transfected with eGFP-REM1.3 (green: REM1.3; red: phalloidin-stained F-actin; bar = 10 μm).

B. F-actin depolymerization prompted collapse of RFs. eGFP-REM1.3-transfected HEK-293 cells were treated with the depolymerization reagent cytochalasin B (1 μg/ml) for 15 min (green: REM1.3; red: phalloidin-stained F-actin; blue: DNA; DMSO: solvent control; CBB: cytochalasin B, bar = 10 μm).

C. SIM image of eGFP-REM1.3-transfected HEK-293 cell (green: REM1.3; red: phalloidin-stained F-actin; blue: DNA; bar = 10 μm).

D. N-STORM images of eGFP-Remorin and Actin-mCherry co-transfected HEK-293 cell stained by activator-reporter paired secondary antibodies (green: 405-647; red: Cy3-647; bar = 10 μm).

E. C-STORM images eGFP-Remorin-transfected HEK-293 stained by a GFP antibody and ALEXA-647-labeled secondary antibody (green: REM1.3; red: phalloidin-stained F-actin; bar = 100 nm).
F. Comprehensive TEM images of RFs. Fluorescein and nano-gold particle double-labeled secondary antibodies were used to stain RFs in HEK293 cells. Fluorescence signal was collected by confocal microscopy and then analyzed by TEM (green: REM1.3; gray: TEM).

Fig 4. Structure-function relationship and biogenesis of RFs.

A. Remorin truncated mutation pattern diagram, the number represents the amino acid position, C represents cysteine.
B. Remorin truncated mutated HEK293 cells (green: REM1.3; red: phalloidin-stained F-actin; blue: DNA; bar = 10 μm).
C. Predicted structures of REM1.3 protein docking to actin oligomer from PDB (1ATN, 1J6Z, 3EL2 and 4A7N).
D. Western blot results of the extracts of lipid microdomains from remorin-truncated mutant transfected HEK293 cells. The upper panel is the sucrose gradient. IN is an unisolated start sample. The 5% and 35% interfaces where the lipid microdomains locate are indicated by arrow; the right panel indicates the antibodies used: eGFP (eGFP).
E. Remorin in animal cells is co-localized with lipid microdomains. Remorin-expressing HEK293 cells were stained for the lipid microdomain marker protein caveolin-1 (CAV1) and cavin-1 (green: REM1.3; red: CAV1 or Cavin-1; blue: DNA; bar = 10 μm).
F. Image subtraction of GFP-REM1.3-transfected Cos7 cells by video microscope (gray: REM1.3; bar = 10 μm). G. Pattern diagram of remorin budding out the vesicle.

Fig 5. Model of RFs biogenesis and the similarity between the migrasome and plasmodesmata.

A. A structural cartoon of RFs. RFs are single- or multiple-microfilament structures formed by remorin on the surface of mammalian cells. As seen from the thumbnail on the right, the green remorin and red actin filaments form a double helix. Remorin interacts with the lipid microdomains on the cell membrane (PM) due to its palmitoylation. Therefore, we speculate that the lipid microdomains (Lipid MD) on the surface of the RFs are also helically distributed. The RFs head has remorins congregation, presumably the center responsible for extending the RFs. On the left is an enlarged fine structure model.

B. A schematic diagram of RFs biogenesis. Remorin modification by palmitoyltransferase is the first step. The second step is remorin and cholesterol-rich cell membrane forming lipid microdomains. In the third step, remorin and lipid microdomains form multimers with actin. In the fourth step, as the RFs polymerize, they begin to extend further to form long RFs.

C. Morphological model diagram of PD and animal RFs or migrasome. Morphologically, PD are prominent membrane vesicles with a filamentous appearance and can be considered a kind of tube connecting the endoplasmic reticulum (ER) of two cells across the cell wall [2, 11-14]. Migrasome or RFs encapsulate the inner-membrane system or cytoplasm and present an expanded beads morphology. Each expanded bead can be seen as a cell of plant, and the plant has cell wall, so it can be that the cell wall pulls the shape of the expanded bead into a cube as a plant cell morphology. Dotted line boxes indicated that plant cells similar to migrasome.

Fig 1

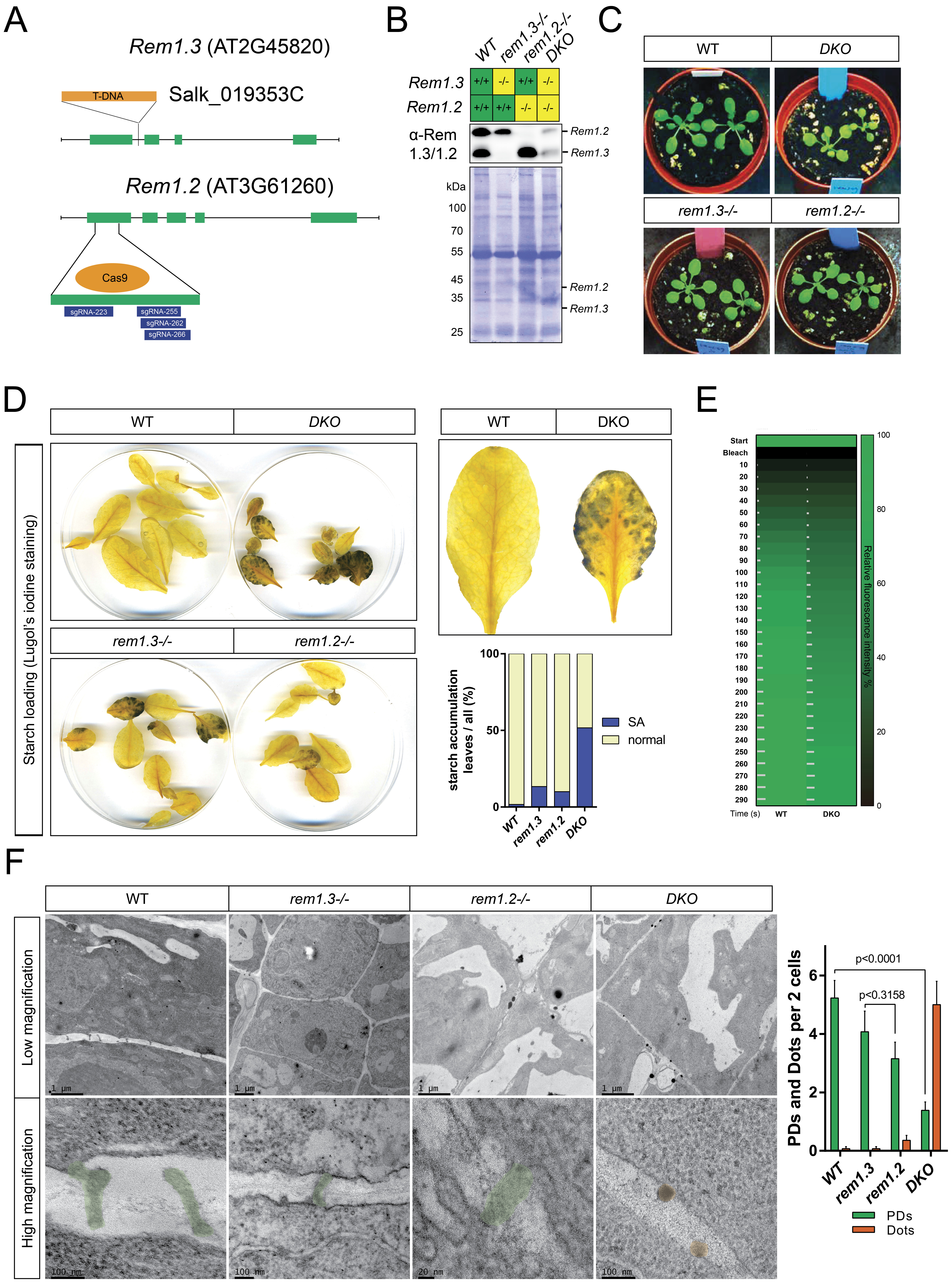
A
Rem1.3 (AT2G45820)
T-DNA
Salk_019353C
Rem1.2 (AT3G61260)
Cas9
sgRNA-223
sgRNA-255
sgRNA-262
sgRNA-266
B
WT
rem1.3-/-
rem1.2-/-
DKO
Rem1.3
Rem1.2
+/+
-/-
α-Rem
1.3/1.2
Rem1.2
Rem1.3
kDa
100
70
55
45
35
25
C
WT
DKO
rem1.3-/-
rem1.2-/-
D
WT
DKO
rem1.3-/-
rem1.2-/-
Starch loading (Lugol's iodine staining)
starch accumulation leaves / all (%)
100
50
0
SA
normal
WT
rem1.3
rem1.2
DKO
E
Start
Bleach
10
20
30
40
50
60
70
80
90
100
110
120
130
140
150
160
170
180
190
200
210
220
230
240
250
260
270
280
290
Time (s)
WT
DKO
Relative fluorescence intensity %
100
80
60
40
20
0
F
WT
rem1.3-/-
rem1.2-/-
DKO
Low magnification
High magnification
1 µm
100 nm
20 nm
PDs and Dots per 2 cells
6
4
2
0
p<0.0001
p<0.3158
WT
rem1.3
rem1.2
DKO
PDs
Dots

Fig 2

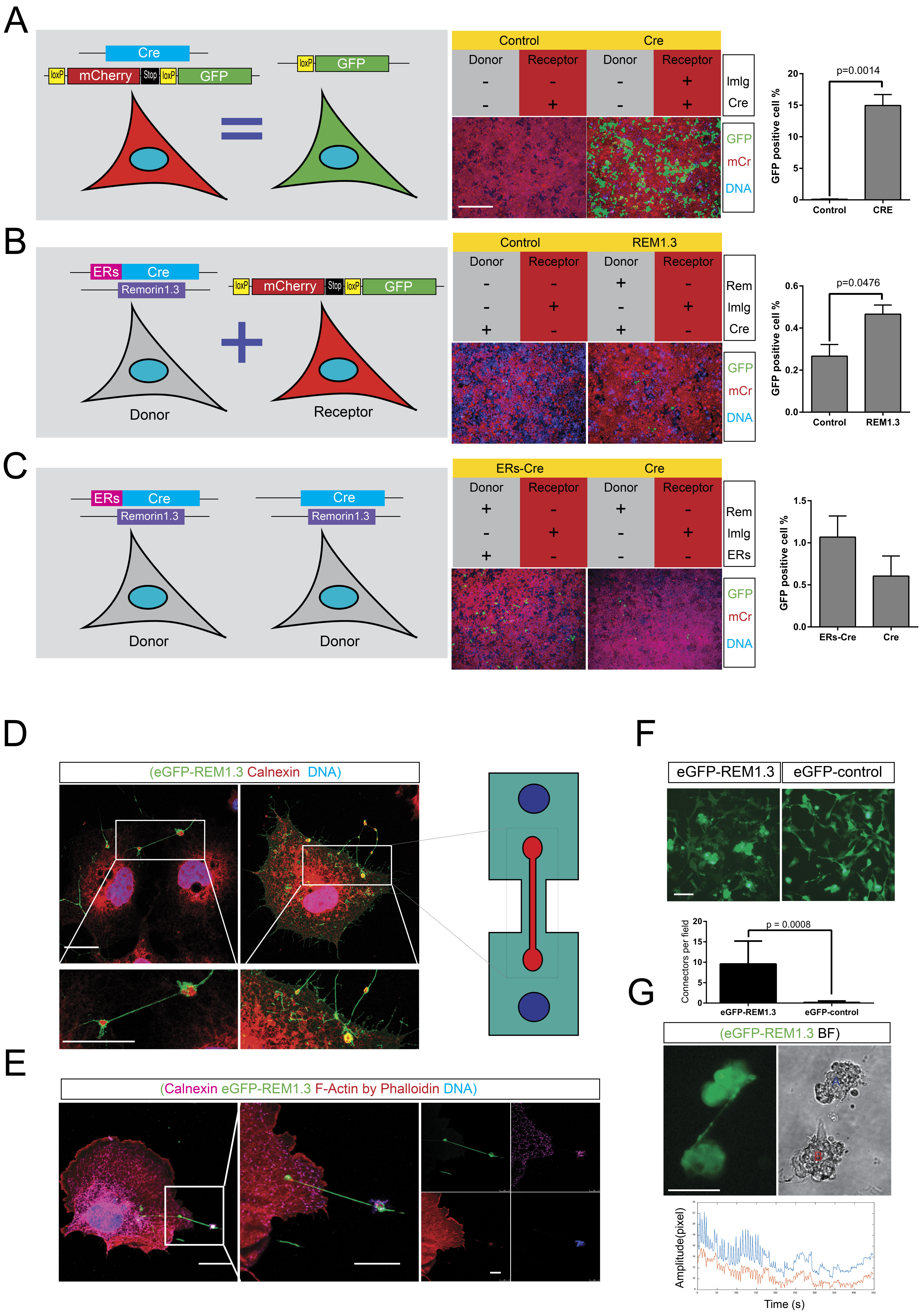
A
Cre
loxP
mCherry
Stop
loxP
GFP
loxP
GFP
Control
Cre
Donor
Receptor
Donor
Receptor
- - - +
- + - +
Imlg
Cre
GFP
mCr
DNA
GFP positive cell %
20
15
10
5
0
p=0.0014
Control
CRE
B
ERs
Cre
Remorin1.3
loxP
mCherry
Stop
loxP
GFP
Donor
Receptor
Control
REM1.3
Donor
Receptor
Donor
Receptor
- - + -
- + - +
+ - + -
Rem
Imlg
Cre
GFP
mCr
DNA
GFP positive cell %
0.6
0.4
0.2
0.0
p=0.0476
Control
REM1.3
C
ERs
Cre
Remorin1.3
Cre
Remorin1.3
Donor
Donor
ERs-Cre
Cre
Donor
Receptor
Donor
Receptor
+ - + -
- + - +
+ - - -
Rem
Imlg
ERs
GFP
mCr
DNA
GFP positive cell %
1.5
1.0
0.5
0.0
ERs-Cre
Cre
D
(eGFP-REM1.3 Calnexin DNA)
E
(Calnexin eGFP-REM1.3 F-Actin by Phalloidin DNA)
F
eGFP-REM1.3
eGFP-control
Connectors per field
20
15
10
5
0
p = 0.0008
eGFP-REM1.3
eGFP-control
G
(eGFP-REM1.3 BF)
A
B
Amplitude(pixel)
Time (s)

Fig 3

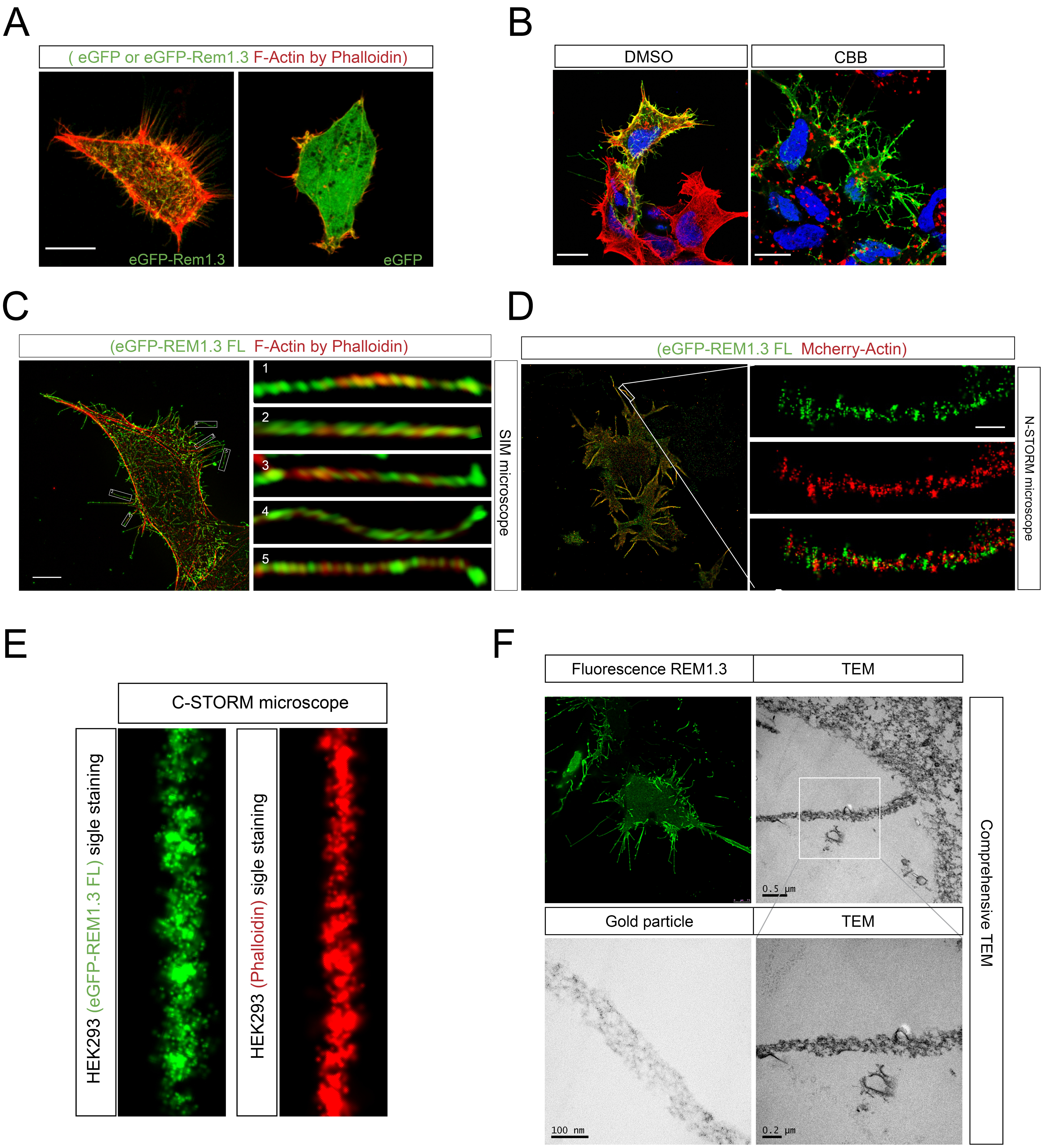
A
(eGFP or eGFP-Rem1.3 F-Actin by Phalloidin)
eGFP-Rem1.3
eGFP
B
DMSO
CBB
C
(eGFP-REM1.3 FL F-Actin by Phalloidin)
1
2
3
4
5
SIM microscope
D
(eGFP-REM1.3 FL Mcherry-Actin)
N-STORM microscope
E
C-STORM microscope
HEK293 (eGFP-REM1.3 FL) sigle staining
HEK293 (Phalloidin) sigle staining
F
Fluorescence REM1.3
TEM
0.5 µm
Gold particle
TEM
100 nm
0.2 µm
Comprehensive TEM

Fig 4

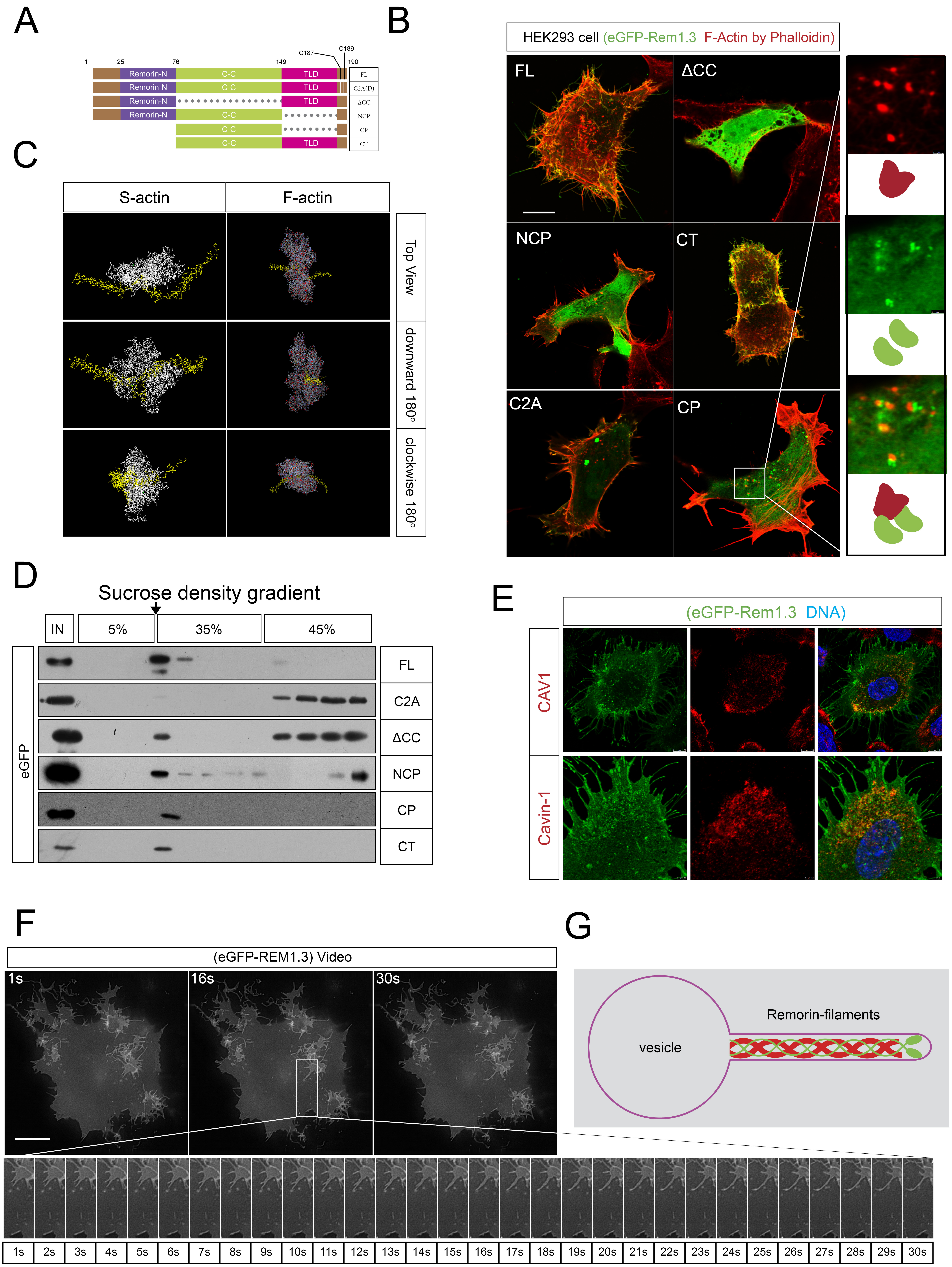
A
C187
C189
1
25
76
149
190
Remorin-N
C-C
TLD
FL
C2A(D)
ΔCC
NCP
CP
CT
B
HEK293 cell (eGFP-Rem1.3 F-Actin by Phalloidin)
FL
ΔCC
NCP
CT
C2A
CP
C
S-actin
F-actin
Top View
downward 180°
clockwise 180°
D
Sucrose density gradient
IN
5%
35%
45%
eGFP
FL
C2A
ΔCC
NCP
CP
CT
E
(eGFP-Rem1.3 DNA)
CAV1
Cavin-1
F
(eGFP-REM1.3) Video
1s
16s
30s
1s 2s 3s 4s 5s 6s 7s 8s 9s 10s 11s 12s 13s 14s 15s 16s 17s 18s 19s 20s 21s 22s 23s 24s 25s 26s 27s 28s 29s 30s
G
Remorin-filaments
vesicle

Fig 5

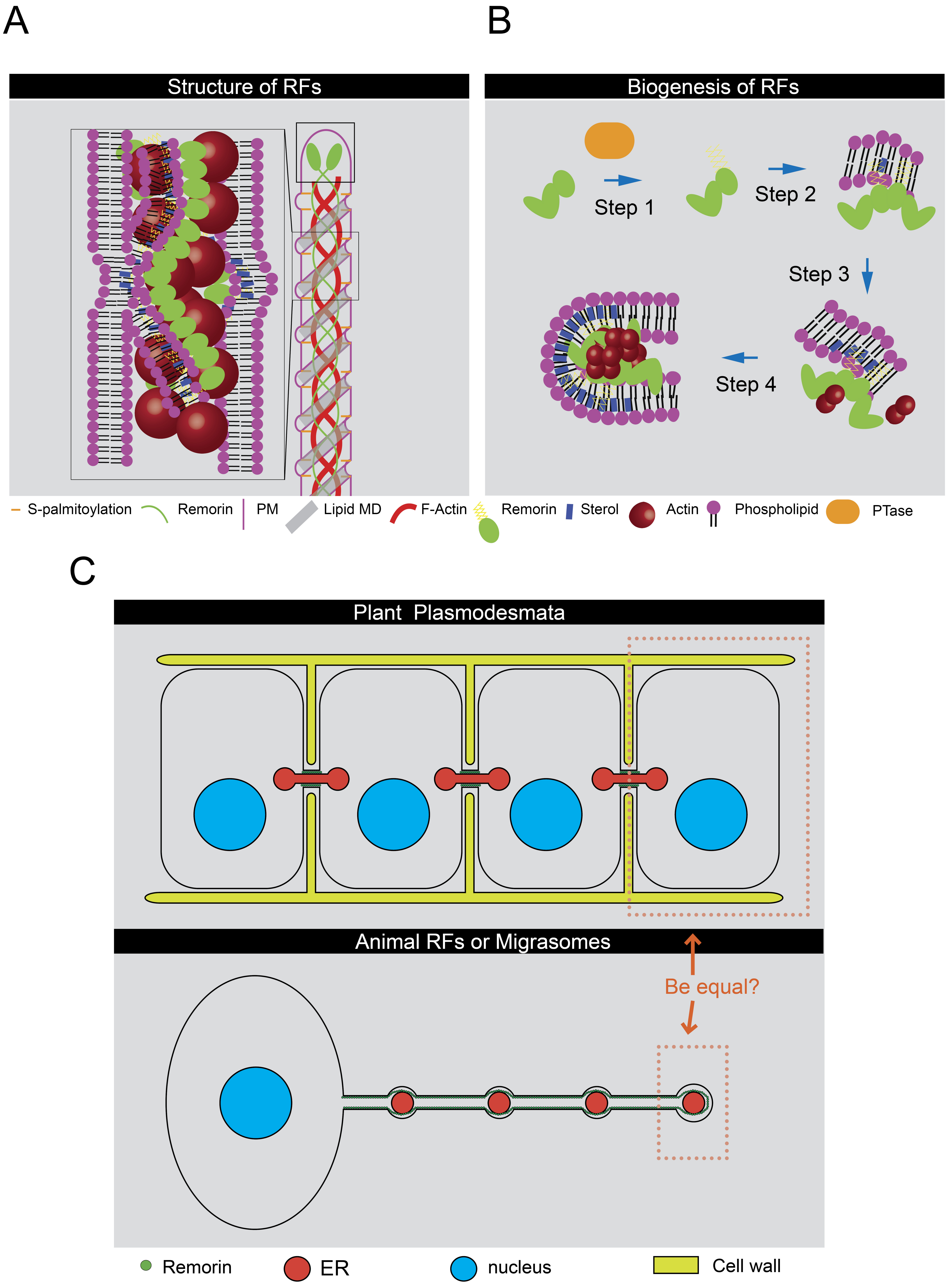
A
B
Structure of RFs
Biogenesis of RFs
Step 1
Step 2
Step 3
Step 4
S-palmitoylation
Remorin
PM
Lipid MD
F-Actin
Remorin
Sterol
Actin
Phospholipid
PTase
C
Plant Plasmodesmata
Animal RFs or Migrasomes
Be equal?
Remorin
ER
nucleus
Cell wall